Infrared Spectra and Density Functional Theory Calculations of Group V Transition Metal Sulfides

Binyong Liang and Lester Andrews*

Department of Chemistry, University of Virginia, P.O. Box 400319, Charlottesville, Virginia 22904-4319

Received: October 11, 2001; In Final Form: January 4, 2002

Laser-ablated vanadium, niobium, and tantalum atoms react with discharged sulfur vapor during co-condensation in excess argon. The primary reaction products are metal disulfides, while evidence for metal monosulfides is found. The ν_1 and ν_3 modes for VS_2, NbS_2, and TaS_2 in argon matrices are observed at 527.8 and 583.5 cm^{-1}, 525.1 and 531.0 cm^{-1}, 523.4 and 516.5 cm^{-1}, respectively. On the bases of the isotopic ν_3 vibrations, the bond angles of VS_2, NbS_2, and TaS_2 are estimated to be 113 ± 3°, 107 ± 3°, and 107 ± 3°. DFT calculations have been performed on the metal sulfides and disulfides, and excellent agreement between the observed and calculated frequencies supports the product identifications.

I. Introduction

Transition metal sulfur compounds are important for both biochemical and industrial catalysis.[1] On one hand, the removal of heteroatoms such as sulfur, nitrogen and metals from oil feedstock by transition metal based catalysts has long been one of the major catalytic processes in the petroleum industry. The removal of sulfur reduces the amount of sulfur oxides released into the atmosphere during the combustion of hydrocarbon fuels and sulfur poisoning of precious metal-based reforming catalysts that are used in producing high octane gasoline. On the other hand, metal sulfides are catalytically active themselves, the deposits of metal sulfides may even increase the activity of a catalyst. In the case where metal sulfides exhibit less catalytic reactivity than their corresponding oxides or bare metals, they are often less susceptible to poisoning and can show higher selectivity.[2]

Vanadium group sulfides have attracted immense interest in the past few years. Bulk vanadium sulfides on their own, particularly V_2S_3, are efficient catalysts for hydrodesulfurization, hydrodenitrogenation, and hydrogenation of aromatic molecules.[3] Both vanadium and niobium sulfides are also used as dopants in other transition-metal-based hydroprocessing catalysts to modify activity and selectivity.[4−7] Moreover, studies have shown superconductivity in a tertiary metal sulfide, $SrTa_2S_5$.[8,9]

Understanding the catalytic bulk metal sulfide chemistry at a molecular level starts at investigating the intrinsic properties of isolated metal sulfide molecules. Vanadium sulfide cations (VS_n^+, $n = 1-10$) have been studied using various mass spectrometric methods and DFT calculations.[10−13] For neutral sulfide species, an earlier argon matrix study reacting transition metal atoms and OCS reported vibrations of VS and VS_2.[14] A very recent laser-induced fluorecence investigation identified the $C^4\Sigma^- \rightarrow X^4\Sigma^-$ band system of VS.[15] Theoretical calculations predicted $^4\Sigma^-$ ground states for VS and NbS, which have similar bonding as their oxide counterparts.[16,17] High-resolution spectroscopy of TaS has been reported, and 17 electronic transitions have been rotationally analyzed.[18] To our knowledge, neither experimental nor theoretical studies have been performed for niobium and tantalum disulfides. We report here a combined IR and DFT investigation of group V sulfides.

II. Experimental and Computational Methods

Sulfur atoms and small molecules were generated by a microwave discharge in argon seeded with sulfur vapor. The coaxial quartz discharge tube is similar to the one used in earlier sulfur experiments.[19] Natural isotopic sulfur (Electronic Space Products, Inc., recrystallized) and enriched sulfur (98% ^{34}S, EG and G Mound Applied Technologies) were used as received; a 50/50 mixture of the two samples was also employed. The vapor pressure of sulfur located in the sidearm was controlled by the resistively heated windings. The microwave discharge was sustained in the argon−sulfur mixture by a Burdick MW220 diathermy (operated at 30−50% of the maximum power level) with an Evenson−Broida cavity and extended from a region about 5 cm downstream of the sulfur reservoir to the end of the discharge tube. The presence of significant quantities of S_2 in the discharge was indicated by the sky-blue emission,[20] different from the normal pink argon discharge.

The experimental method for laser ablation and matrix isolation has been described in detail previously.[21−23] Briefly, the Nd:YAG laser fundamental (1064 nm, 10 Hz repetition rate with 10 ns pulse width, 3−20 mJ/pulse) was focused to ablate the rotating vanadium (Alfa, 99.5%), niobium (Johnson-Mathey, 99%) or tantalum (Mackay, 99.99%) metal target. Laser-ablated metal atoms were co-deposited with the sulfur-doped argon spray-on stream onto a 7 K CsI window at 2−4 mmol/h for 0.5−1.5 h. Infrared spectra were recorded at 0.5 cm^{-1} resolution on a Nicolet 550 spectrometer with 0.1 cm^{-1} accuracy using a mercury cadmium telluride detector down to 400 cm^{-1}. Matrix samples were annealed at different temperatures, and selected samples were subjected to irradiation using a medium-pressure mercury lamp ($\lambda > 240$ nm) with the globe removed.

DFT calculations were performed on group V metal mono- and disulfides using the GAUSSIAN 98 program[24] and the B3LYP[25] functional. The 6-311+G* basis set was used for sulfur and vanadium,[26] and the LanL2DZ effective core potential and basis set was employed for niobium and tantalum.[27]

III. Results

Infrared Spectra. Cocondensation of laser-ablated V, Nb, Ta metal atoms with a sulfur-seeded argon discharge stream

10.1021/jp013790n CCC: $22.00
Published on Web 03/19/2002

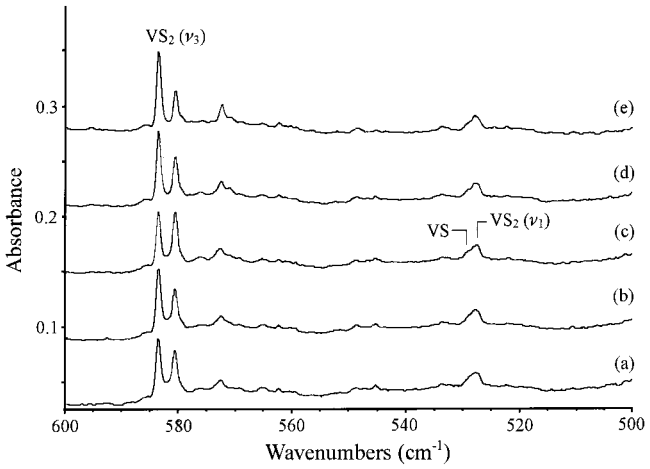

Figure 1. Infrared spectra in the 600−500 cm^{-1} region for laser-ablated V co-deposited with discharged S in argon at 7 K. (a) sample deposited for 60 min, (b) after 25K annealing, (c) after $\lambda > 240$ nm irradiation, (d) after 35 K annealing, (e) after 40 K annealing.

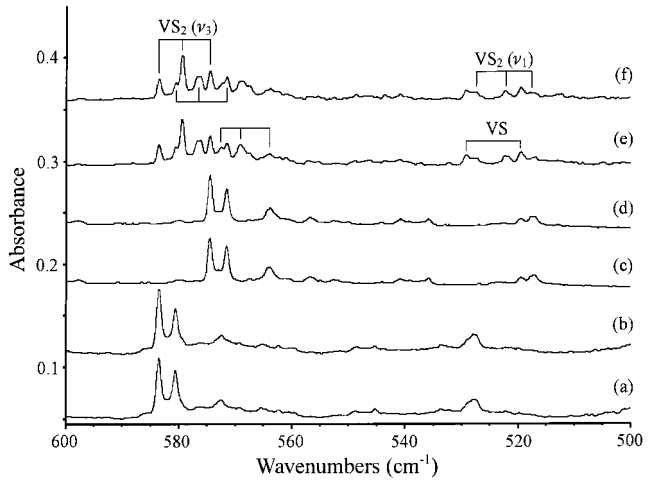

Figure 2. Infrared spectra in the 600−500 cm^{-1} regions for laser-ablated V co-deposited with discharged S in argon at 7 K. (a, b) ^{32}S, (c, d) ^{34}S, (e, f) 50/50 $^{32}S + {}^{34}S$ mixture. Spectra (a, c, e) recorded after sample deposition; spectra (b, d, f) recorded after 25 K annealing.

produced common bands in the infrared spectra. These common bands[19] include absorptions of S_3 at 679.8 and 676.0 cm^{-1}, S_4 at 661.7 and 642.4 cm^{-1}, CS_2 at 1528.0 cm^{-1}, and weak S_2O at 1157.1 cm^{-1}. The spectral regions showing distinct new features are presented in the Figures 1−6, and the absorption bands in different ^{34}S and mixed $^{32}S + {}^{34}S$ isotopic experiments are listed in the Table 1. Complementary experiments were done with each metal and an Ar/OCS sample. The product bands in different experiments, and their assignments will be described in the next section.

DFT Calculations. The ground-state configurations of S, V, Nb, and Ta atoms were reproduced as $[Ne]3s^23p^4$, $[Ar]3d^34s^2$, $[Kr]4d^45s^1$, and $[Xe]4f^{14}5d^36s^2$, respectively. The calculation on S_2 and S_3 found ground states of $^3\Sigma_g^-$ and $^1A_1$, respectively. The S−S bond length in the S_2 molecule is 1.927 Å, whereas in the S_3 molecule, the S−S bond length is 1.952, and the bond angle is 118.2°. For comparison valance angle calculations from four pairs of symmetrical isotopic ν_3 values gave 116 ± 2° for S_3.[19] For every metal mono- and disulfide, calculations were performed on doublet and quartet spin multiplicities. For metal disulfides, both linear and bent starting geometries were employed. We also commonly switched occupied and virtual orbitals to confirm that the state under consideration was in fact

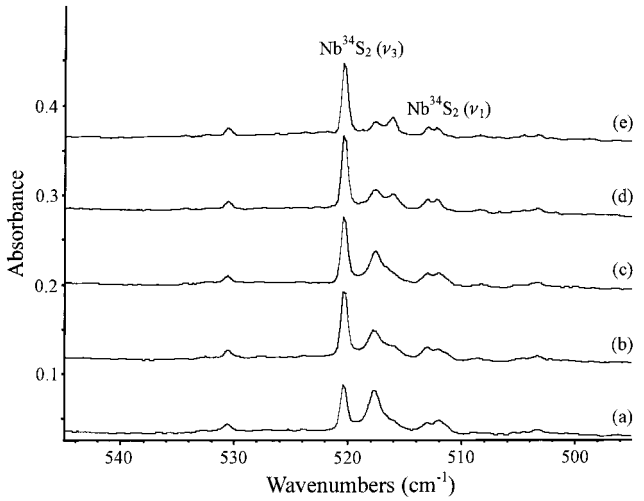

Figure 3. Infrared spectra in the 545−495 cm^{-1} region for laser-ablated Nb co-deposited with discharged ^{34}S in argon at 7 K. (a) sample deposited for 60 min, (b) after 25K annealing, (c) after $\lambda > 240$ nm irradiation, (d) after 35 K annealing, (e) after 40 K annealing.

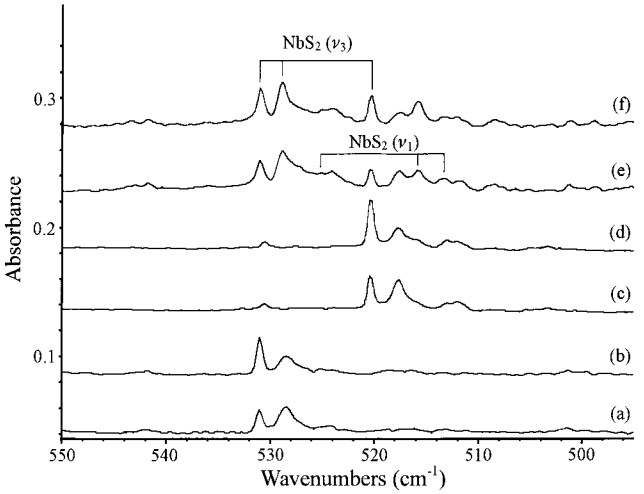

Figure 4. Infrared spectra in the 550−495 cm^{-1} regions for laser-ablated Nb co-deposited with discharged S in argon at 7 K. (a, b) ^{32}S, (c, d) ^{34}S, (e, f) 50/50 $^{32}S + {}^{34}S$ mixture. Spectra (a, c, e) recorded after sample deposition; spectra (b, d, f) recorded after 25 K annealing.

the ground state. Analytical second-derivatives were used to obtain the harmonic frequencies. The ground states for both VS and NbS are $^4\Sigma^-$ ($\delta^2\sigma^1$), whereas the ground state of TaS is $^2\Delta$ ($\delta^1\sigma^2$). These results are similar to their oxide counterparts.[16,17,28] The ground states for all three disulfides are bent $^2A_1$, this is also in accord with their oxide counterparts. Although an earlier DFT/B3LYP calculation on VO_2 reported a $^2B_1$ ground state,[29] reinvestigation with the same type of calculation reveals that the $^2A_1$ state is 1.0 kcal/mol lower in energy than the $^2B_1$ state. The detailed calculation results for the ground and low-lying excited states of metal mono and disulfides, and new results for VO_2 are summarized in the Tables 2−4.

IV. Discussion

The group V transition metal sulfides will be assigned in turn.

VS. Absorption at 528 cm^{-1} was resolved into two bands at 529.2 and 527.8 cm^{-1} on annealing to 35 K (Figure 1d). The upper band at 529.2 cm^{-1} is assigned to the VS fundamental. In the isotopic ^{34}S experiment, the 529.2 cm^{-1} band is shifted to 519.7 cm^{-1}, which is clearly resolved from the ^{34}S counterpart of the 527.8 cm^{-1} band at 517.1 cm^{-1} (Figure 2c,d). The

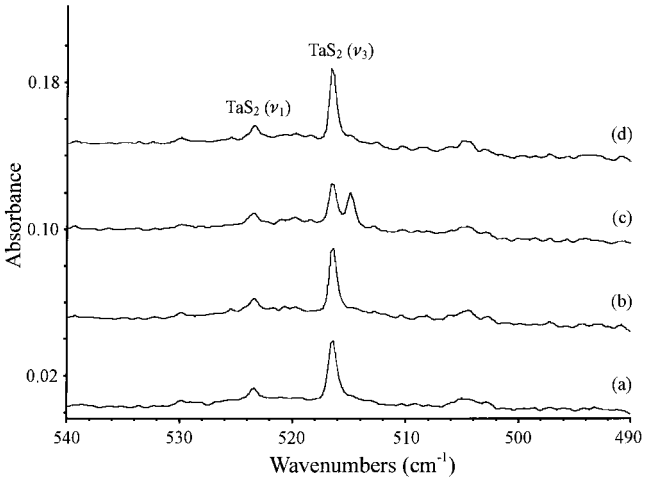

Figure 5. Infrared spectra in the 540−490 cm^{-1} region for laser-ablated Ta co-deposited with discharged S in argon at 7 K. (a) sample deposited for 50 min, (b) after 25K annealing, (c) after $\lambda > 240$ nm irradiation, (d) after 35 K annealing.

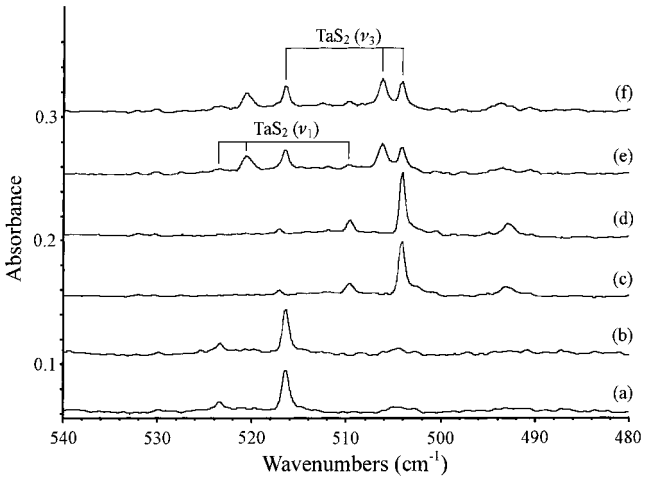

Figure 6. Infrared spectra in the 540−480 cm^{-1} regions for laser-ablated Ta co-deposited with discharged S in argon at 7 K. (a, b) ^{32}S, (c, d) ^{34}S, (e, f) 50/50 $^{32}S + {}^{34}S$ mixture. Spectra (a, c, e) recorded after sample deposition; spectra (b, d, f) recorded after 25 K annealing.

$^{32}S/^{34}S$ isotopic frequency ratio of 1.0183 is very close to the harmonic diatomic ratio of 1.0186 for VS. The mixed isotopic $^{32}S + {}^{34}S$ experiment gave only two pure isotopic absorptions, which confirmed that a single sulfur atom is involved in this vibrational mode (Figure 2 e,f). The 529.2 cm^{-1} argon matrix VS fundamental is in excellent agreement with the first vibronic band separation of 542.1 cm^{-1} recently observed in the gas phase.[15] This matrix shift, 12.9 cm^{-1}, is smaller than the matrix shift (17.9 cm^{-1}) observed[29] for VO at 983.6 cm^{-1}, but the VS matrix shift is a larger percentage, 2.4%, as compared to 1.8% for VO.

In the DFT calculation, the ground electronic state of VS is predicted as $^4\Sigma^-$, with a $\delta^2\sigma^1$ configuration. The lowest doublet state $^2\Sigma^-$ is 20.5 kcal/mol higher in energy. The vibrational analysis for the $^4\Sigma^-$ state predicted a harmonic V−S stretching mode (ω_e) at 537.1 cm^{-1}, which is in excellent agreement with the matrix observation and requires a scale factor of 0.985. Our DFT calculation also agrees with earlier higher level MCPF and CCSD(T) calculations[16] on VS: the DFT bond length is within 0.02 Å, and ω_e is within 17 cm^{-1}.

In a previous study of first-row transition-metal sulfides using the thermal V + OCS reaction,[14] a band at 584 cm^{-1} was assigned to VS and a stronger 530 cm^{-1} band to VS_2 without support from isotopic substitution. These assignments are incorrect: the stronger 530 cm^{-1} product band is due to VS, as might be expected, and the absorption at 584 cm^{-1} will be reassigned to VS_2 in the next paragraph. The present OCS experiment gave a sharp band at 529.3 cm^{-1} ($A = 0.019$), which is due to VS, and another band at 532.0 cm^{-1} which may be due to VS perturbed by CO; no band was observed near 580 cm^{-1}. It is interesting to note that VO was observed at 983.1 cm^{-1} with 10% of the intensity of VS. Other product bands at 537.9, 974.8, 1881.2 and 1980.9 cm^{-1} are probably due to inserted OCVS or OVCS species that are beyond the scope of this investigation.[23] Finally, a weak 529.2 cm^{-1} band was observed for VS in a similar experiment with CS_2 precursor.

TABLE 1: Infrared Absorptions (cm^{-1}) from Codeposition of Laser-Ablated V, Nb, and Ta Atoms with Discharged Sulfur in Excess Argon

^{32}S	^{34}S	$^{32}S + {}^{34}S$	R(32/34)	identity
		Vanadium		
583.5	574.5	583.6, 579.5, 574.5	1.0157	VS_2, ν_3
580.6	571.6	580.5, 576.2, 571.5	1.0157	VS_2 site, ν_3
572.5	563.8	572.5, 568.5, 563.8	1.0154	VS_2 site, ν_3
529.2	519.7	529.2, 519.7	1.0183	VS
527.8	517.1	527.8, 522.3, 517.1	1.0207	VS_2, ν_1
		Niobium		
541.8	530.6		1.0211	(X-NbS_2)
531.0	520.3	531.0, 529.0, 520.3	1.0206	NbS_2, ν_3
528.5	517.7		1.0209	NbS_2 site, ν_3
526.5	516.1	526.5, 523.7, 515.9	1.0201	NbS_2 site, ν_3
525.1	513.0	525.1, 515.8, 513.0	1.0236	NbS_2, ν_1
524.1	512.0		1.0236	NbS_2 site, ν_1
		Tantalum		
529.9	517.1		1.0248	(X-TaS_2)
523.4	509.6	523.4, 520.6, 509.8	1.0271	TaS_2, ν_1
516.5	504.1	516.5, 506.2, 504.1	1.0246	TaS_2, ν_3
514.9	502.6	514.9, 505.1, 502.7	1.0245	TaS_2 site, ν_3
504.8	493.0		1.0239	Ta_xS_y

TABLE 2: Calculated Electronic State, Relative Energy, Geometry, and Frequencies for VS, NbS, and TaS

species	electronic state	relative energy, kcal/mol	geometry, Å	frequency, cm^{-1} (intensity, km/mol)
VS	$^4\Sigma^-$ ($\delta^2\sigma^1$)	0	2.062	537.1(67)
	$^2\Sigma^-$ ($\delta^2\sigma^1$)	+20.5	2.034	579.5(65)
	$^2\Delta$ ($\delta^1\sigma^2$)	+25.8	2.007	572.4(32)
NbS	$^4\Sigma^-$ ($\delta^2\sigma^1$)	0	2.155	541.4(47)
	$^2\Delta$ ($\delta^1\sigma^2$)	+17.7	2.119	575.8(43)
	$^4\Phi$ ($\pi^1\delta^1\sigma^1$)	+18.8	2.191	503.4(64)
	$^2\Sigma^-$ ($\delta^2\sigma^1$)	+19.9	2.146	554.7(41)
TaS	$^2\Delta$ ($\delta^1\sigma^2$)	0	2.121	552.7(19)
	$^4\Sigma^-$ ($\delta^2\sigma^1$)	+4.7	2.152	522.1(27)

VS_2. Two sharp and strong bands at 583.5 and 580.6 cm^{-1} were observed on deposition. The 583.5 cm^{-1} band increased and the 580.6 cm^{-1} band decreased slightly on annealing, whereas opposite behavior was found for UV irradiation (Figure 1). In the isotopic ^{34}S experiment, these two bands shifted to 574.5 and 571.6 cm^{-1}, and both have $^{32}S/^{34}S$ isotopic frequency ratios of 1.0157. In the mixed $^{32}S/^{34}S$ experiment, both bands showed 1/2/1 triplet patterns, which indicates the involvement of two equivalent sulfur atoms in this vibrational mode (Figure 2e,f). Two intermediate bands at 579.5 and 576.2 cm^{-1} are 0.4 and 0.2 cm^{-1}, respectively, *higher* than the medians of the corresponding pure isotopic bands. The 583.5 and 580.8 cm^{-1} absorptions are assigned to the antisymmetric V−S stretching mode of the VS_2 molecule at two different matrix sites. A weak band at 572.5 cm^{-1} showed similar isotopic frequency ratio and triplet splitting pattern in the mixed $^{32}S + {}^{34}S$ experiment. This band is assigned to the antisymmetric V−S stretching mode of

TABLE 3: Calculated Electronic State, Relative Energy, Geometry, and Frequencies for VS_2, NbS_2, TaS_2, and VO_2

species	electronic state	relative energy, kcal/mol	geometry, Å, deg	frequency, cm^{-1} (intensity, km/mol) ν_1	ν_2	ν_3
VS_2	$^2A_1$	0	2.040, 110.8	546.8(8)	180.7(0)	590.5(126)
	$^2B_1$	+17.9	2.100, 171.7	435.9(1)	145.8i(57)	598.1(221)
	$^4B_2$	+24.4	2.120, 106.5	482.3(53)	84.1(8)	262.0(70)
cyclic $V(S_2)$	$^4B_1$	+18.2	2.259, 56.4	498.2(37)	367.0(4)	262.7(8)
	$^2B_1$	+34.8	2.242, 57.0	500.7(51)	380.4(8)	303.4(11)
NbS_2	$^2A_1$	0	2.165, 107.0	536.9(13)	184.4(0)	534.9(113)
	$^2B_1$	+12.9	2.183, 114.5	519.2(12)	153.3(1)	526.2(157)
	$^4A_2$	+34.6	2.234, 101.7	470.1(36)	111.2(2)	204.6(7)
cyclic $Nb(S_2)$	$^4B_1$	+46.6	2.385, 52.6	499.9(28)	341.3(5)	213.5(4)
	$^2B_1$	+58.7	2.374, 53.0	496.1(27)	353.8(9)	223.6(8)
TaS_2	$^2A_1$	0	2.159, 107.9	527.0(8)	174.8(0)	512.3(80)
	$^2B_1$	+23.3	2.183, 114.6	504.6(9)	144.6(0)	488.7(91)
	$^4A_2$	+40.2	2.226, 104.5	459.1(24)	102.5(2)	248.2(22)
cyclic $Ta(S_2)$	$^4B_1$	+66.5	2.368, 53.4	496.6(18)	324.8(6)	231.4(1)
	$^2A_1$	+67.3	2.333, 54.3	509.4(25)	341.6(1)	248.0(1)
VO_2	$^2A_1$	0	1.610, 115.7	1027.6(34)	261.4(4)	997.4(427)
	$^2B_1$	+1.0	1.612, 120.9	1022.7(44)	311.8(16)	1010.9(493)

TABLE 4: Comparison of Computed and Experimental Metal−Sulfur Stretching Frequencies (cm^{-1}) in VS_2, NbS_2, and TaS_2

species	mode	computed $M^{32}S_2$	computed $M^{34}S_2$	computed R(32/34)	exptl $M^{32}S_2$	exptl $M^{34}S_2$	exptl R(32/34)
VS_2	ν_1	546.8	535.9	1.0203	527.8	517.1	1.0207
	ν_3	590.5	581.0	1.0162	583.5	574.5	1.0157
NbS_2	ν_1	536.9	524.4	1.0238	525.1	513.0	1.0236
	ν_3	534.9	523.9	1.0210	531.0	520.3	1.0206
TaS_2	ν_1	527.0	513.2	1.0269	523.4	509.6	1.0271
	ν_3	512.3	499.9	1.0248	516.5	504.1	1.0246

VS_2 in another matrix site. The 527.8 cm^{-1} band is weak compared to the 583.5 and 580.8 cm^{-1} bands, and also partially coincident with the VS absorption at 529.2 cm^{-1}. Fortunately, the two bands are fully resolved in the isotopic ^{34}S experiment (Figure 2c,d), and the ^{34}S counterpart at 517.4 cm^{-1} apparently tracks with the sum of absorbance of 574.5 and 571.6 cm^{-1} bands. The 527.8 cm^{-1} band showed a triplet feature in the mixed $^{32}S/^{34}S$ experiment (Figure 2e,f). The intermediate band at 522.3 cm^{-1} is 0.2 cm^{-1} *lower* than the median of two pure isotopic bands, which is in accord with the blue-shifting of the intermediate $^{32}SV^{34}S$ band of the antisymmetric V−S stretching mode in the VS_2 molecule. The 527.8 cm^{-1} band is hence assigned to the symmetric V−S stretching mode of the VS_2 molecule. It is interesting to note that the average $^{32}S/^{34}S$ isotopic frequency ratio of symmetric and antisymmetric stretching modes (1.0182) is very close to the same value in the diatomic VS molecule (1.0183). The antisymmetric stretching frequencies of VS_2 and $V^{34}S_2$ provide basis for calculation of a 117 ± 3° upper limit to the S−V−S bond angle.[30,31] In the case of MoO_2 where seven natural Mo isotopes and two oxygen isotopes are available, both the valence angle lower limit and upper limit were deduced from various apex and terminal isotopic molecule pairs.[32] Accordingly, the true angle for VS_2 will be on the order of 4° lower than the 117 ± 3° value deduced from sulfur isotopic substitution.

DFT calculations on the VS_2 molecule were performed to support the spectroscopic observations. The ground state is found to be $^2A_1$, with V−S bond length of 2.040 Å and S−V−S bond angle of 110.8°. The lowest quartet state of VS_2, and the doublet and quartet cyclic $V(S_2)$ molecule are at least 17 kcal/mol higher in energy than the $^2A_1$ ground state (Table 3). The vibrational analysis of the $^2A_1$ state predicted ν_1 and ν_3 modes at 546.8 and 590.5 cm^{-1}, with absorption intensities of 8 and 126 km/mol, respectively. These results agree with the experimental values very well. The calculated $^{32}S/^{34}S$ isotopic frequency ratios, for the ν_1 and ν_3 modes, 1.0203 and 1.0162, are very close to the experimental values. The ν_2 mode is predicted at 180.7 cm^{-1} with essentially no infrared absorption intensity. Nevertheless, this band position is out of the detection window of our instrument.

The earlier matrix assignment[14] of absorptions at 622 and 530 cm^{-1} to the ν_1 and ν_3 modes of VS_2 must be revised. This work employed OCS to produce vanadium sulfides, and without isotopic substitution, assigned VS and VS_2 absorptions on the bases of the variations of band intensities on reagent concentrations. In the present mixed $^{32}S/^{34}S$ isotopic experiment, the triplet features for both ν_1 and ν_3 modes at 527.8 and 583.5 cm^{-1} clearly demonstrate the involvement of two equivalent sulfur atoms in the responsible molecule. The asymmetry of the ν_1 and ν_3 triplets further showed that ν_3 is higher in frequency than ν_1. Moreover, the excellent agreement between DFT calculation and the spectroscopic observation confirms the current band assignments.

NbS_2. Two strong bands were observed after deposition: the band at 531.0 cm^{-1} sharpened and increased on annealing, whereas the broader band at 528.5 cm^{-1} gradually decreased on annealings (Figure 4a,b). In the ^{34}S experiment (Figure 3), these two bands appeared at 520.3 and 517.7 cm^{-1}, with $^{32}S/^{34}S$ isotopic ratios of 1.0206 and 1.0209, respectively. In the mixed $^{32}S/^{34}S$ experiment (Figure 4e,f), a triplet is clearly observed for the sharp 531.0 cm^{-1} band with an intermediate band at 529.0 cm^{-1}, whereas for the broader 528.5 cm^{-1} band the splitting pattern is not fully resolved. These two bands are assigned to the antisymmetric stretching mode of NbS_2 in two matrix sites. A third matrix site at 526.5 cm^{-1} is also observed on late annealing. The much weaker ν_1 mode of NbS_2 was observed at 525.1 and 524.1 cm^{-1} in two matrix sites; both red-shifted to 513.0 and 512.0 cm^{-1} with the same $^{32}S/^{34}S$ isotopic frequency ratios (1.0236). Similar to the VS_2 molecule, the average of the ν_1 and ν_3 $^{32}S/^{34}S$ isotopic frequency ratios (1.0222) is close to the harmonic diatomic ratio of 1.0226. In the mixed $^{32}S/^{34}S$ experiment, a triplet splitting pattern was observed for the 525.1 cm^{-1} band with an intermediate band at 515.8 cm^{-1} (Figure 4e,f). Not surprisingly, the interaction of antisymmetric and symmetric S−Nb−S stretching modes in the lower symmetry $^{32}S-Nb-^{34}S$ molecule made both observed triplets asymmetric: the intermediate bands in the ν_3 and ν_1 triplets are blue-shifted 3.4 cm^{-1} and red-shifted 3.3 cm^{-1}, respectively, from the medians of their pure isotopic counterparts. It is noteworthy that the closeness of ν_1 and ν_3 frequencies leads to the stronger interaction between two intermediate bands

compared to the VS_2 counterparts. On the bases of the $^{32}S/^{34}S$ isotopic frequencies of the ν_3 mode, the upper limit of the S−Nb−S bond angle is deduced as 111 ± 3°. Similarly, the true angle will be near 107 ± 3°.

The ground NbS_2 state is predicted as $^2A_1$ in DFT calculations with the Nb−S bond length of 2.165 Å and the S−Nb−S bond angle of 107.0°. Other low-lying states have at least 12 kcal/mol higher energies, and the $^4B_1$ state cyclic $Nb(S_2)$ is 46.6 kcal/mol higher. The predicted ν_1 and ν_3 modes for the $^2A_1$ ground state are at 536.9 and 534.9 cm^{-1} with absorption intensities of 13 and 113 km/mol, respectively. These results agree with the experimental values fairly well, except that the predicted ν_1 mode absorbs at a slightly higher frequency than the ν_3 mode, whereas the opposite was found experimentally. The calculated isotopic frequency ratios also agree with the observed values (Table 4). The ν_2 mode is predicted at 184.4 cm^{-1}, and it is out of our detection window.

TaS_2. Similar to the VS_2 and NbS_2 molecules, both ν_1 and ν_3 modes for the TaS_2 molecule were observed. The strong absorption at 516.5 cm^{-1} observed on deposition is assigned to the antisymmetric stretching mode of TaS_2 (Figure 5). In the ^{34}S isotopic experiment (Figure 6c,d), this band shifted to 504.1 cm^{-1} with a $^{32}S/^{34}S$ isotopic frequency ratio of 1.0246. The weaker absorption at 523.4 cm^{-1} is assigned to the ν_1 mode of TaS_2; this band shifted to 509.6 cm^{-1} with an isotopic frequency ratio of 1.0271 (Figure 6). The average of ν_1 and ν_3 isotopic frequency ratios again is very close to the harmonic diatomic value of 1.0259. The 514.9 cm^{-1} band is only observed after UV irradiation (Figure 5c), and it showed a similar isotopic frequency ratio and splitting pattern as those of the 516.5 cm^{-1} band. The 514.9 cm^{-1} band is assigned to the ν_3 mode of TaS_2 molecule at another matrix site. In the mixed $^{32}S/^{34}S$ experiment, both ν_1 and ν_3 modes split into triplets (Figure 6e,f), and the intermediate bands are blue-shifted 4.0 cm^{-1} and red-shifted 4.1 cm^{-1}, respectively, from the medians of their corresponding pure isotopic bands. The S−Ta−S bond angle upper limit calculated from the $Ta^{32}S_2$ and $Ta^{34}S_2$ isotopic frequencies is 111 ± 3°, and the true angle will be near 107 ± 3°.

DFT calculations on TaS_2 predicted the ground state as $^2A_1$, whereas other low-lying states are at least 23 kcal/mol higher, and the $^4B_1$ state cyclic $Ta(S_2)$ is 66.5 kcal/mol higher in energy. The calculated bond length is 2.159 Å, and the bond angle is 107.9°. The ν_1 and ν_3 vibrational modes are predicted at 527.0 and 512.3 cm^{-1}, with absorption intensities of 8 and 80 km/mol, respectively. These results are in very good agreement with the experimental values. The predicted isotopic ratios listed in the Table 4 also agree well with the observed values. The ν_2 mode is computed at 114.8 cm^{-1}, and it is out of our detection window.

Other Absorptions. In the niobium experiment, a weak band at 541.8 cm^{-1} compared to the NbS_2 ν_3 mode shifted to 530.6 cm^{-1} in the ^{34}S experiment (Figure 4). In the mixed $^{32}S/^{34}S$ experiment, although the strong NbS_2 ν_3 band covers the spectral region around 531.0 cm^{-1}, this band appears to have an intermediate component near 536 cm^{-1}. The DFT calculation on NbS produced a ground state of $^4\Sigma^-$ with a $\delta^2\sigma^1$ configuration, and the calculated 541.4 cm^{-1} harmonic frequency is very close to the observed value. However, the isotopic frequency ratio of 1.0211 is lower than the harmonic diatomic ratio of 1.0226, but the ratio is almost that found for the ν_3 mode of NbS_2 (1.0206). We tentatively assign this band to an antisymmetric $Nb-S_2$ mode in a higher niobium sulfide species.

The Nb experiment with OCS gave less intense products than the V investigation, and a weak new 508.7 cm^{-1} band is probably due to the OCNbS insertion product, but we cannot be certain without isotopic substitution.

In the tantalum experiment, a similar weak band observed at 529.9 cm^{-1} shifted to 517.1 cm^{-1} in the ^{34}S experiment. In the mixed $^{32}S + {}^{34}S$ experiment, the band splitting pattern is not clear (Figure 6). This band is in the region expected for TaS. The DFT calculation predicted the ground state as $^2\Delta$, whereas the $^4\Sigma^-$ state is only 4.7 kcal/mol higher in energy. The frequency analysis predicted the harmonic vibration at 552.7 cm^{-1}, which is in excellent agreement with a recent gas phase determination[18] of the $X^2\Delta$ state TaS fundamental as 549.2 cm^{-1}. However, the isotopic frequency ratio of 1.0248 is lower than the harmonic diatomic ratio of 1.0259, but close to the value for ν_3 of TaS_2 (1.0246). This band is probably due to a similar $Ta-S_2$ mode in a higher sulfide. A Ta experiment with OCS yielded still weaker product absorptions than Nb and no absorption in the 500 cm^{-1} region.

A weak band observed at 504.8 cm^{-1} on deposition in the Ta experiment increased slightly on annealing (Figure 5). The $^{32}S/^{34}S$ isotopic frequency ratio of 1.0239 is even lower than the ratio for the ν_3 mode of TaS_2. The isotopic splitting pattern could not be resolved in the mixed isotopic experiment due to the weak nature of the band. The band is possibly due to a higher tantalum sulfide; we generically assign it to Ta_xS_y, where x and y are small integers.

Reaction Mechanisms. Possible reactions for product formation, along with zero-point-energy-corrected relative energy changes calculated by DFT are

$$M + S \rightarrow MS \quad (1)$$

($\Delta E = -102.5$, -116.2, and -119.3 kcal/mol for V, Nb, and Ta)

$$M + S_2 \rightarrow MS + S \quad (2)$$

($\Delta E = -9.4$, -23.1, and -26.2 kcal/mol for V, Nb, and Ta)

$$M + S_3 \rightarrow MS + S_2 \quad (3)$$

($\Delta E = -57.7$, -71.4, and -74.5 kcal/mol for V, Nb, and Ta)

$$M + S_2 \rightarrow MS_2 \quad (4)$$

($\Delta E = -95.3$, -127.0, and -142.6 kcal/mol for V, Nb, and Ta)

$$M + S_3 \rightarrow MS_2 + S \quad (5)$$

($\Delta E = -50.5$, -82.2, and -97.8 kcal/mol for V, Nb, and Ta)

The ΔE values for the reaction 1 are actually $-D_0$ values for the MS molecules. Only D_0 for VS has been measured experimentally, and our calculated value (103 kcal/mol) is near the reported value (106 kcal/mol).[33]

In the current experiment, the dominant processes for formation of MS and MS_2 cannot be determined. Although all five proposed reactions are thermodynamically favored for all three metals, no apparent increase of the metal sulfide bands was observed during the annealing and irradiation cycles in the matrices. This result suggests that the formations of MS and MS_2 require significant amount of activation energies. Metal

sulfides are only formed during the laser-ablation processes when the ablated metal atoms provide sufficient activation energies to overcome the reaction barriers.[34] Reactions 2 and 4 are probably most important as S_2 is expected to be the major sulfur reagent, although its concentration could not be measured, and MS_2 is the dominant product.

Comparison of V, Nb, and Ta Monosulfides. Bonding in the first-row transition-metal monosulfides is similar to bonding in the oxide counterparts.[16] In the case of vanadium monosulfide, the $^4\Sigma^-$ ($\delta^2\sigma^1$) ground state is derived from ionic, $V^+(3d\sigma^1 3d\delta^2 4s^1)$-$S^-(3p\sigma^1 3p\pi^4)$, and covalent, $V(3d\sigma^1 3d\pi^1 3d\delta^2 4s^1)S(3p\sigma^1 3p\pi^3)$, components. The σ bonding is formed between the vanadium hybridized dsσ and the sulfur 3pσ orbital electrons, with another nonbonding dsσ electron polarizing away from sulfur. The π bonding is between vanadium 3dπ and sulfur 3pπ orbitals: in the ionic limit it is the sulfur $3p\pi^4$ electrons donating to the empty 3dπ orbitals, whereas in the covalent limit it is the electron pairing between 3dπ and 3pπ orbital electrons. Two electrons in vanadium 3dδ orbitals are essentially nonbonding, and do not affect bonding.

A similar bonding scheme can be applied to NbS and TaS. Our DFT calculation predicted the same $^4\Sigma^-$ ground state for NbS, however for TaS, the ground state was calculated as $^2\Delta$ instead, and the $^4\Sigma^-$ state lies 4.7 kcal/mol higher in energy. The reversal of the electronic states in TaS can be attributed to the relativistic effect for the third-row transition metals, which substantially stabilize the 6s orbital of the tantalum atom. As a result, the energy separation of $d^4s^1-d^3s^2$ in Ta (1.21 eV) is significantly higher than in V (0.26 eV),[35] and TaS stays low spin. In fact, the niobium atom has the ground-state electronic configuration of $4d^45s^1$, which suggests that NbS should have a larger covalent bonding character than VS.

V. Conclusions

Laser-ablated vanadium, niobium, and tantalum atoms react with discharged sulfur vapor during co-condensation in excess argon. The absorptions of VS and MS_2 (M = V, Nb. Ta) have been observed, and confirmed by the isotopic substitution. Isotopic mixtures ($^{32}S + {}^{34}S$) are required to discriminate between VS and VS_2. The VS fundamental in solid argon is redshifted 12.9 cm^{-1} from the gas-phase value.[15] The ν_1 and ν_3 modes for VS_2, NbS_2, and TaS_2 absorb at 527.8 and 583.5 cm^{-1}, 525.1 and 531.0 cm^{-1}, 523.4 and 516.5 cm^{-1}, respectively, in solid argon. Based on the isotopic ν_3 vibrations, the bond angles of VS_2, NbS_2, and TaS_2 are estimated to be 113 ± 3°, 107 ± 3°, and 107 ± 3°. DFT calculations on metal mono- and disulfides give frequencies in excellent agreement with the observed values and support the product identifications.

A brief comparison with the group V dioxides and disulfides can be made: all have the ground $^2A_1$ state and the valence angles of VO_2 and VS_2 (114° and 113 ± 3°), NbO_2, NbS_2, TaO_2 and TaS_2 (107 ± 3°) are the same for each metal (Table 3, ref. 28,29). The ν_3 frequencies of the disulfides are 62, 61 and 57% of the ν_3 frequencies for VO_2, NbO_2 and TaO_2, respectively.[28,29] Thus the group V dioxide and disulfide molecules are similar.

Acknowledgment. The authors gratefully acknowledge National Science Foundation support from Grant CHE 00-78836.

References and Notes

(1) Stiefel, E. I., Matsumoto, K., Eds. *Transition Metal Sulfur Chemistry, Biological and Industrial Significance*; American Chemical Society: Washington, DC, 1997.

(2) Weber, T., Prins, R., van Santen, R. A., Eds. *Transition Metal Sulphides, Chemistry and Catalysis*; NATO ASI Series; Kluwer Academic Publishers: Dordrecht, Netherlands, 1998.

(3) Guillard, C.; Lacroix, M.; Vrinat, M.; Breysse, M.; Mocaer, B.; Grimblot, J.; des Courieres, T.; Faure, D. *Catal. Today* **1990,** *7,* 587.

(4) Scott, C. E.; Embaid, B. P.; Gonzalez-Jimenez, F.; Hubaut, R.; Grimblot, J. *J. Catal.* **1997**, *166*, 333.

(5) Geantet, C.; Afonso, J.; Breysse, M.; Allali, N.; Danot, M. *Catal. Today* **1996**, *28*, 23.

(6) Yumoto, M.; Kukes, S. G.; Klein, M. T.; Gates, B. C. *Ind. Eng. Chem. Res.*, **1996**, *35*, 3203.

(7) Gaborit, V.; Allali, N.; Geantet, C.; Breysse, M.; Vrinat, M.; Danot, M. *Catal. Today* **2000**, *57*, 267.

(8) Kijima, N.; Morie, K.; Nagata, S.; Shimono, I. *J. Low Temp. Phys.* **1996**, *105*, 1511.

(9) Kijima, N.; Takahashi, M.; Matsumoto, N.; Nagata, S. *J. Solid State Chem.* **1998**, *135*, 325.

(10) Carlin, T. J.; Wise, M. B.; Freiser, B. S. *Inorg. Chem.* **1981**, *20*, 2743.

(11) Dance, I.; Fisher, K.; Willett, G. *Angew. Chem., Int. Ed. Engl.* **1995**, *34*, 201.

(12) Dance, I. G.; Fisher, K. J.; Willett, G. D. *Inorg. Chem.* **1996**, *35*, 4177.

(13) Kretzschmar, I.; Schröder, D.; Schwarz, H.; Rue, C.; Armentrout, P. B. *J. Phys. Chem. A* **1998**, *102*, 10060.

(14) DeVore, T. C.; Franzen, H. F. *High Temp. Sci.* **1975**, *7*, 220.

(15) Cheng, A. S. C. *J. Chin. Chem. Soc.* **2001**, *48*, 283.

(16) Bauschlicher, C. W., Jr.; Langhoff, S. R. *J. Chem. Phys.* **1986**, *85*, 5936. Bauschlicher, C. W., Jr.; Maitre, P. *Theor. Chim. Acta* **1995**, *90*, 189.

(17) Langhoff, S. R.; Bauschlicher, C. W., Jr. *J. Chem. Phys.* **1988**, *89*, 2160.

(18) Wallin, S.; Edvinsson, G.; Taklif, A. G. *J. Mol. Spectrosc.* **1997**, *184*, 466. *J. Mol. Spectrosc.* **1998**, *192*, 368.

(19) Brabson, G. D.; Mielke, Z.; Andrews, L. *J. Phys. Chem.* **1991**, *95*, 79.

(20) Long, S. R.; Pimentel, G. C. *J. Chem. Phys.* **1977**, *66*, 2219. Smardzewski, R. R. *J. Chem. Phys.* **1978**, *68*, 2878.

(21) Burkholder, T. R.; Andrews, L. *J. Chem. Phys.* **1991**, *95*, 8697.

(22) Hassanzadeh, P.; Andrews, L. *J. Phys. Chem.* **1992**, *96*, 9177.

(23) Zhou, M. F.; Andrews, L. *J. Phys. Chem A.* **2000**, *104*, 4394.

(24) Frisch, M. J.; Trucks, G. W.; Schlegel, H. B.; Scuseria, G. E.; Robb, M. A.; Cheeseman, J. R.; Zakrzewski, J. A.; Montgomery, J. A.; Stratmann, R. E.; Burant, J. C.; Dapprich, S.; Millam, J. M.; Daniels, A. D.; Kudin, K. N.; Strain, M. C.; Farkas, O.; Tomasi, J.; Barone, V.; Cossi, M.; Cammi, R.; Mennucci, B.; Pomelli, C.; Adamo, C.; Clifford, S.; Ochterski, J.; Petersson, G. A.; Ayala, P. Y.; Cui, Q.; Morokuma, K.; Malick, D. K.; Rabuck, A. D.; Raghavachari, K.; Foresman, J. B.; Cioslowki, J.; Ortiz, J. V.; Stefanov, B. B.; Liu, G.; Liashenko, A.; Piskorz, P.; Komaromi, I.; Gomperts, R.; Martin, R. L.; Fox, D. J.; Keith, T.; Al-Laham, M. A.; Peng, C. Y.; Nanayakkara, A.; Gonzalez, C.; Challacombe, M.; Gill, P. M. W.; Johnson, B. G.; Chen, W.; Wong, M. W.; Andres, J. L.; Head-Gordon, M.; Replogle, E. S.; Pople, J. A. *Gaussian 98*, revision A.1.; Gaussian, Inc.: Pittsburgh, PA, 1998.

(25) Lee, C.; Yang, E.; Parr, R. G. *Phys. Rev. B* **1988**, *37*, 785.

(26) McLean, A. D.; Chandler, G. S. *J. Chem. Phys.* **1980**, *72*, 5639. Wachters, A. J. H.; *J. Chem. Phys.* **1970**, *52*, 1033. Hay, P. J. *J. Chem. Phys*. **1977**, *66*, 4377. K. Raghavachari, K.; Trucks, G. W. *J. Chem. Phys.* **1989**, *91*, 1062.

(27) Hay, P. J.; Wadt, W. R. *J. Chem. Phys.* **1985**, *82*, 270. Wadt, W. R.; Hay, P. J. *J. Chem. Phys.* **1985**, *82*, 284. Hay, P. J.; Wadt, W. R. *J. Chem. Phys.* **1985**, *82*, 299.

(28) Zhou, M. F.; Andrews, L. *J. Phys. Chem. A* **1998**, *102*, 8251 (Nb, Ta + O_2).

(29) Chertihin, G. V.; Bare, W. D.; Andrews, L. *J. Phys. Chem. A* **1997**, *101*, 5090 (V + O_2).

(30) Allavena, M.; Rysnik, R.; White, D.; Calder, V.; Mann, D. E. *J. Chem. Phys.* **1969**, *50*, 3399.

(31) Andrews, L. *J. Elect. Spectrosc.* **1998**, *97*, 63.

(32) Bare, W. D.; Souter, P. F.; Andrews, L. *J. Phys. Chem. A* **1998**, *102*, 8279.

(33) Huber, K. P.; Herzberg, G. *Constants of Diatomic Molecules*; Van Nostrand Reinhold: New York, 1979.

(34) Kang, H.; Beauchamp, J. L. *J. Phys. Chem.* **1985**, *89*, 3364.

(35) Moore, C. E. Atomic Energy Levels. U. S. National Bureau of Standards Circular 467; U. S. Government Printing Office: Washington, DC, 1958.